

Estimate black hole masses of AGNs using ultraviolet emission line properties

Min-Zhi Kong^{1,2}*, Xue-Bing Wu², Ran Wang² and Jin-Lin Han¹

¹ National Astronomical Observatories, Chinese Academy of Sciences, Beijing 100012, China

² Department of Astronomy, Peking University, Beijing 100871, China

Received; accepted

Abstract Based on the measured sizes of broad line region of the reverberation-mapping AGN sample, two new empirical relations are introduced to estimate the central black hole masses of radio-loud high-redshift ($z > 0.5$) AGNs. First, using the archival *IUE/HST* spectroscopy data at UV band for the reverberation-mapping objects, we obtained two new empirical relations between the BLR size and MgII /CIV emission line luminosity. Secondly, using the newly determined black hole masses of the reverberation-mapping sample for calibration, two new relationships for determination of black hole mass with the full width of half maximum and the luminosity of MgII /CIV line are also found. We then apply the relations to estimate the black hole masses of AGNs in Large Bright Quasar Survey and a sample of radio-loud quasars. For the objects with small radio-loudness, the black hole mass estimated using the $R_{BLR} - L_{MgII/CIV}$ relation is consistent with that from the $R_{BLR} - L_{3000\text{\AA}/1350\text{\AA}}$ relation. But for radio-loud AGNs, the mass estimated from the $R_{BLR} - L_{MgII/CIV}$ relation is systematically lower than that from the continuum luminosity $L_{3000\text{\AA}/1350\text{\AA}}$. Because jets could have significant contributions to the UV/optical continuum luminosity of radio-loud AGNs, we emphasized again that for radio-loud AGNs, the emission line luminosity may be a better tracer of the ionizing luminosity than the continuum luminosity, so that the relations between the BLR size and UV emission line luminosity should be used to estimate the black hole masses of high redshift radio-loud AGNs.

Key words: galaxies: nucleus – galaxies: high-redshift – quasars: emission lines – Ultraviolet: galaxies

1 INTRODUCTION

Black hole masses of high-redshift AGNs ($z \gtrsim 1$) are essential to understand the early history of the universe and the formation of supermassive black holes. The mass of black hole can be estimated by $M_{BH} \sim R_{BLR} V^2 / G$ assume that gas around a black hole is virialized. Here V is the characteristic velocity of BLR gas at distance R_{BLR} from the center of a AGN (Peterson & Wandel 1999; Peterson 1993), G is the gravitational constant. The velocity can be estimated from V_{FWHM} (full width at half maximum) of emission lines. For randomly distributed BLR clouds, $V = (\sqrt{3}/2)V_{FWHM}$. The exact scale factor between V and V_{FWHM} depends on the structure, kinematics, and orientation of BLR (Peterson & Wandel 1999, 2000; McLure & Dunlop 2001; Wu & Han et al. 2001; Zhang & Wu, 2002). Taking practical parameters, the virial mass of a black hole can thus be expressed in the form of (see Kaspi et al. 2000)

$$M_{BH} = 1.464 \times 10^5 \left(\frac{R_{BLR}}{\text{lt} - \text{days}} \right) \left(\frac{V_{FWHM}}{10^3 \text{ km s}^{-1}} \right)^2 M_{\odot}.$$

The reverberation mapping technique is the most important method to study the geometry and kinematics of gas in BLR (Blandford & McKee 1982; Peterson 1993, 1999, 2000; Horne et al. 2004). The BLR size, R_{BLR} , can be deduced from time delay of luminosity variations of broad emission lines, often $H\beta$ emission line (see Peterson et al. 2004 and references therein), relative to that of ionizing continuum. In principle, this technique can be applied to any AGN. In practice, monitor observations of AGNs for the time delay are very time-consuming as it can have a time scale of weeks, months or even years. Up to now, only 20 Seyfert 1 galaxies and 17 nearby quasars (Kaspi et al. 2000; Wandel et al. 1999; Peterson et al. 1998; Santos-Lleo et al. 2001) have been well monitored in the reverberation-mapping studies.

To ease the problem, Kaspi et al. (2000) first successfully obtained an empirical relation between BLR sizes of AGNs in the reverberation mapping sample and optical continuum luminosities at 5100 \AA , i.e. the $R_{BLR} - \lambda L_{\lambda}(5100 \text{ \AA})$ relation, which can be used to estimate BLR size. Peterson et al. (2004) recently have re-analyzed the reverberation mapping data for 35 AGNs (after PG 1351+640 and PG 1704+608 were omitted) and obtained the improved time delays and hence BLR sizes and black home masses. Using the improved BLR sizes in Peterson et al.(2004) and the new cosmological model, Kaspi et al. (2005) recently investigated the relation between BLR sizes and luminosities of $H\beta$ line and continuum at 5100 \AA , 1450 \AA , 1350 \AA and 2-10 keV. Specifically, they found $R_{BLR} \propto \lambda L_{\lambda}(5100 \text{ \AA})^{0.67 \pm 0.05}$ with about 40% intrinsic scatter. The mass of black hole

of a low-redshift ($z \lesssim 0.8$) AGN can thus be easily estimated using the above relation on R_{BLR} and V_{FWHM} (Laor 2000; McLure & Dunlop et al. 2001; Wandel 2002; Wu & Liu 2004). For objects at higher redshift ($0.8 \lesssim z \lesssim 2.5$), as McLure & Jarvis (2002) stated, V_{FWHM} of MgII can be adopted to substitute for V_{FWHM} of $H\beta$, mainly because they both are strong, fully permitted and low-ionization lines with similar ionization potentials and are emitted at approximately the same radius from the central ionizing source. It is not surprising that the FWHM values for MgII and $H\beta$ are very closely related for reverberation mapping objects. McLure & Jarvis (2002) obtained a relation between the R_{BLR} from $H\beta$ time lag and the continuum luminosity $\lambda L_{\lambda}(3000\text{\AA})$. Note, however, a spectrum near 3000\AA is seriously contaminated by the blended FeII and the Balmer continuum, so it is important to remove their effects when measuring the FWHM of MgII. The FeII emission can be removed from the continuum by model-fitting (McLure & Dunlop 2004), while the Balmer continuum contribution is not obvious in the residual spectrum and difficult to remove. For two AGN samples, LBQS (Forster et al. 2001) and the Molonglo quasar sample (Kapahi et al. 1998), McLure & Jarvis (2002) calculated the black hole masses using the two relations, $R_{BLR} - \lambda L_{\lambda}(5100\text{\AA})$ and $R_{BLR} - \lambda L_{\lambda}(3000\text{\AA})$, and found that results agree well with each other.

For a given object, NGC 5548, Peterson & Wandel (1999) found from time delay of different emission lines that the same virial relationship exists for lines emitted at different distances from the central black hole, such as $H\beta$, CIV $\lambda 1549$, HeII $\lambda 1640$. Similar results have been obtained also for NGC 7469 and 3C 390.3 (Peterson & Wandel 2000). This suggests a possibility to determine the black hole mass using the line properties and/or continuum luminosity at short wavelength around CIV $\lambda 1549$ (Vestergaard 2002). To estimate the velocity, as Vestergaard (2002) pointed out, the FWHM of CIV can be used because the line is available for large redshift range between $z \sim 1 - 5$ and not much affected by strong absorption lines and the FeII emission. To estimate the R_{BLR} , Kaspi et al. (2005) has got the $R_{BLR} - \lambda L_{\lambda}(1350\text{\AA})$ and $R_{BLR} - \lambda L_{\lambda}(1450\text{\AA})$ relations with a power index about 0.55 ± 0.05 . Using the $R_{BLR}(H\beta) - L$ relation and the FWHM of CIV, one can estimate black hole mass. The mass estimates can be calibrated using the reverberation mapping results because the BLR size of CIV and $H\beta$ are probably different.

In most cases, the observed continuum luminosity of an AGN is mainly contributed from its nucleus. But some fraction of the continuum comes from the nonthermal emission of jet and host galaxy. Especially for radio-loud quasars and BL Lac objects, jets could contribute significantly to the continuum radiation. Jet emission has so far been detected in all kinds of radio sources at optical/UV/X-ray/ γ -ray band (Jester 2003). More than ten UV/optical jets have been found (O'Dea, et al. 1999; Scarpa & Urry 2002; Parma et al. 2003; Scarpa et al. 1999). To diminish the jet contribution, as well as the continuum radiation from host galaxies (though it is much weaker than the AGN), the line luminosity

should be used to deduce the $R_{BLR} - L$ relation. Wu et al. (2004) have suggested a new relation between the BLR size and the $H\beta$ emission line luminosity, and have shown that, for radio-loud AGNs, black hole masses estimated using such a new relation are systematically lower than those derived using the $R_{BLR} - \lambda L_{\lambda}(5100\text{\AA})$ relation. We noticed that the relations for R_{BLR} with the continuum luminosity, as obtained in Kaspi et al. (2005), were deduced from the 35 reverberation mapping AGNs. Most of them are radio-quiet objects and only five of them, including PG 1704+608, with radio-loudness greater than 10 and only one object, PG 1226+023 (3C 273), have radio-loudness greater than 1000 (see Nelson 2000). Therefore the presence of a few radio-loud objects only has minor effect to the $R-L$ relationships. The $R-L$ relation derived from the reverberation mapping AGN sample therefore is not the best to estimate black hole masses of radio-loud objects for the reasons we mentioned above.

Similar to that of $H\beta$ line, the $MgII$, CIV line luminosities may be the better tracers to the ionizing luminosity for radio-loud AGNs than the UV continuum luminosities. Although the detailed line radiation mechanisms are different, with $H\beta$ being a recombination line and $MgII$, CIV being collisionally excited lines, these three lines are all permitted lines produced by the photo-ionization process. Therefore we expect that the luminosities of these lines can all trace the ionizing luminosity but with different calibration factors. In fact, we have investigated the correlations between the $MgII$, CIV line luminosities and the continuum luminosities or $H\beta$ line luminosity for the reverberation mapping AGNs, and found that the correlation coefficients are all greater than 0.9.

The main purpose of this work is to find relations between the BLR size and the $MgII$, CIV emission line luminosity which can be used to estimate black hole mass for high-redshift radio-loud AGNs. We will compare the black hole masses obtained using, respectively, the relation between the BLR size and the UV line luminosity, and that between the BLR size and the UV continuum luminosity, and then examine whether the black hole masses for radio-loud high-redshift objects are systematically overestimated using the UV continuum luminosity.

In Sect.2, we present the spectral measurements of the $MgII$, CIV emission lines obtained from archival UV data of *IUE/HST* observations for the reverberation-mapping AGNs. In Sect.3, we investigate the relations between the BLR size and $MgII$, CIV emission line luminosity using data for the reverberation-mapping AGNs. In Sect.4, we apply the relations to other AGN samples for black hole mass estimation, and compare the black hole masses obtained by using different relations. In Sect.5, we present our conclusions and discussions.

Throughout the paper, a cosmological model, with $H_0 = 70 \text{ km s}^{-1} \text{ Mpc}^{-1}$, $\Omega_{\Lambda} = 0.7$, $\Omega_M = 0.3$, has been adopted.

2 DATA FOR THE REVERBERATION-MAPPING AGNS

To investigate possible relations between the BLR size and MgII , CIV emission line luminosity, we collect data for reverberation-mapping AGNs. We take the average BLR size values for 35 AGNs in Peterson et al. (2004) obtained from the time delay of H β line. There is no systematically measurements of the luminosities of MgII , CIV emission lines for reverberation-mapping AGNs in the literature. We have measured them ourselves using the UV spectra from the IUE or HST archive. The spectra of most objects are available from *IUE*, and a few from *HST*. We measured the MgII emission lines for 27 objects and CIV emission lines for 33 objects.

Data reduction consists of several steps. First, all AGN spectra have been extinction-corrected following a method given by Cardelli et al. (1989) and shifted to the rest frame using the IRAF software. Secondly iron emission features in each spectrum were subtracted and the continuum is fitted with a power-law. Thirdly the FWHM and the flux of MgII and CIV emission lines were measured.

2.1 Iron emission subtraction and continuum fitting

Without subtraction of iron emission in UV/optical spectra of AGNs, the accuracy of measurements of emission lines as well as the continua (Boroson & Green 1992; Corbin & Boroson 1996; Vestergaard & Wilkes 2001) would be limited, particularly for MgII profile because it is often blended by relative strong FeII around 2800Å.

Assuming the relative strength of iron lines (i.e. a template) are the same for all AGNs, Boroson & Green (1992) have developed a method to fit and remove iron lines in optical spectra (in the rest frame) of quasars. Vestergaard & Wilkes (2001) developed an iron template in the UV band from 1250Å to 3090Å (in the rest frame) using HST spectra of a narrow line Seyfert galaxy, I Zwicky 1, which has rich iron emission lines. They found that the template works well for eliminating the iron emissions from spectra of a few quasars. We followed the similar procedures as Vestergaard & Wilkes (2001) to subtract the iron emission using their iron template, and simultaneously fit a power law to several continuum windows from 1000 Å to 3100 Å without obvious emission lines or *Feii* emissions (see Table 2 from Kuraszkiwicz et al. 2002). We finally determined the flux at 3000Å or 1350Å from iron-subtracted spectrum.

2.2 CIV and MgII emission line measurements

Now we try to obtain the emission line properties from the clean-spectrum that both the iron emissions and the fitted continuum were subtracted.

We normally use only one Gaussian component to fit the CIV /MgII line profile and obtain FWHM, if there is no an obvious narrow component. One component usually can

provide a good description of line profile, especially for MgII . However, if an absorption line is blended with CIV or MgII lines, such as in NGC 4151, PG 1411+442, another Gaussian absorption component is added in fitting. We ignore the asymmetry of CIV profiles often seen in subtracted spectra, which may be induced by a relative broad emission line such as HeII λ 1640 and OIII] λ 1663 in the red-wing or an absorption line in the blue-wing, as we believe that their net effect in fitting result is small. We measure the line width from each spectrum, and then take the average for the FWHM of MgII and CIV emission lines (see Columns 4 and 7 in Table 1). We adopted an uncertainty of 20 percent if only one spectrum is available for an object. We did not measure and take the line dispersion (the second moment of the profile) as an alternative to the FWHM, which was suggested by Peterson et al. (2004) and Fromerth & Melia (2000), mainly because the line dispersion agrees well with the FWHM in the limit of a Gaussian line profile. As mentioned above, in most cases of our measurements one Gaussian component can provide a satisfactory fit to the line profile. Fluxes obtained by direct integration over the observed emission line profile of the clean-spectrum were adopted.

In Table 1, we list all data used or obtained in this paper. The columns are object name (1), R_{BLR} (2) and the black hole mass (3) from Peterson et al. (2004), the FWHM (4) and luminosity (5) of MgII , the luminosity of continuum at 3000 \AA (6), the FWHM (7) and luminosity (8) of CIV , the continuum luminosity at 3000 \AA (9). Data from column (4) to column (9) are our measurements (see the following sections), and the number of the good spectra used is given in columns (10) and (11) with marks indicating which archive of the spectra.

3 NEW EMPIRICAL RELATIONS FOR BLACK HOLE MASS ESTIMATIONS

We first try to establish the relations between the BLR size and the luminosity of MgII , CIV emission line, using data of the reverberation mapping AGNs obtained above. These relations can be used to estimate the BLR size of high-redshift AGNs from measurements of the luminosity of MgII , CIV emission line, as we will do in the next section. Together with the BLR velocity obtained from the line-width, the black hole masses of high-redshift AGNs can be estimated. In this section, we will also use the known masses of black holes of the reverberation mapping AGNs to “calibrate” the empirical relations.

3.1 Relationships between the BLR size and MgII , CIV emission line luminosity of the reverberation AGNs

We take the value of the BLR size of the reverberation mapping sample from Peterson et al. (2004) and the UV line luminosities measured above to investigate their relations. As shown in Fig. 1 for the MgII line luminosities of 27 AGNs and Fig. 2 for the CIV line

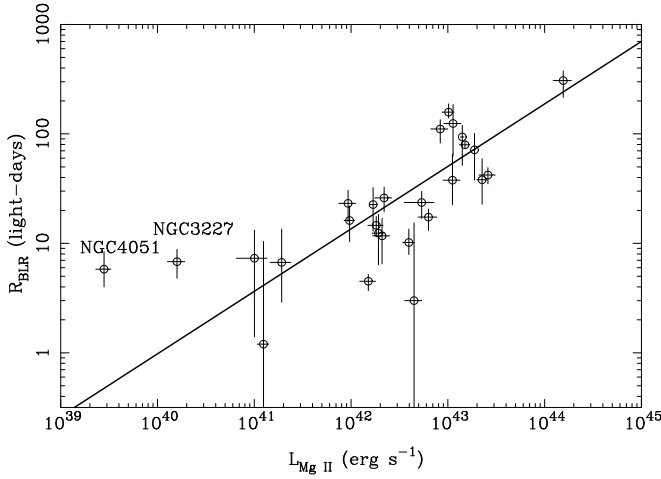


Fig. 1 The BLR size, R_{BLR} , versus the luminosity of MgII emission line ($\lambda 2798 \text{ \AA}$), L_{MgII} , of 27 AGNs in the reverberation mapping sample for which the MgII emission line have been measured in Sect.2. The correlation coefficient between the two parameters is 0.72. The solid line shows an OLS bisector fit to data (Eq. 1), and has a slope of 0.57.

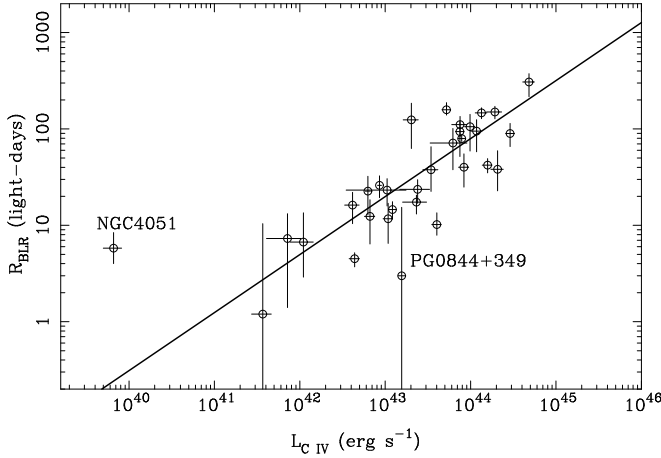


Fig. 2 The same as Fig.1, but for the CIV emission line ($\lambda 1549 \text{ \AA}$) of 33 AGNs. The correlation coefficient is 0.76. The solid line (Eq. 2) has a slope of 0.60.

luminosities of 33 AGNs, the BLR size and the line luminosities are closely related, with the correlation coefficients of 0.72 and 0.76, respectively. The best fitted lines with the OLS bisector method (Isobe et al. 1990) are

$$\log \frac{R_{BLR}}{\text{lt.days}} = (1.13 \pm 0.13) + (0.57 \pm 0.12) \log \left(\frac{L_{MgII}}{10^{42} \text{erg s}^{-1}} \right), \quad (1)$$

$$\log \frac{R_{BLR}}{\text{lt.days}} = (0.69 \pm 0.28) + (0.60 \pm 0.16) \log \left(\frac{L_{CIV}}{10^{42} \text{erg s}^{-1}} \right). \quad (2)$$

Given the uncertainties, the slopes are slightly larger than but still consistent with the value 0.5 expected from a simple photo-ionization model for the BLR.

We also investigated the relations between the R_{BLR} and the continuum luminosity $\lambda L_{3000\text{\AA}}$ or $\lambda L_{1350\text{\AA}}$ using our measurements in Table 1, and obtained the following relations,

$$\log \frac{R_{BLR}}{\text{lt.days}} = (1.27 \pm 0.10) + (0.58 \pm 0.10) \log\left(\frac{L_{3000\text{\AA}}}{10^{44}\text{erg s}^{-1}}\right), \quad (3)$$

$$\log \frac{R_{BLR}}{\text{lt.days}} = (1.15 \pm 0.14) + (0.56 \pm 0.12) \log\left(\frac{L_{1350\text{\AA}}}{10^{44}\text{erg s}^{-1}}\right). \quad (4)$$

The correlation coefficients are 0.72 and 0.75, respectively. For the relationship between R_{BLR} and $L_{3000\text{\AA}}$, the slope of 0.58 ± 0.10 we obtained is consistent with 0.47 ± 0.05 derived by McLure & Jarvis (2002) from 34 reverberation AGNs (Kaspi et al. 2000). The relationship between R_{BLR} and $L_{1350\text{\AA}}$ was obtained recently by Kaspi et al. (2005) for the first time from measurements, with a slope of 0.56 ± 0.05 from the BCES method and 0.50 ± 0.04 from the *fitexy* method. Our slope of 0.56 ± 0.12 is well consistent with their value.

There is a well-known relationship between the equivalent width of CIV broad emission line and the 1350\AA continuum luminosity of AGNs (Baldwin 1977). This so-called Baldwin-effect can be converted to $L_{CIV} \propto L_{1350\text{\AA}}^\alpha$, with a typical value of $\alpha \sim 0.4$ for an individual AGN but $\alpha \sim 0.83 \pm 0.04$ for a sample of AGNs (see Peterson 1997 and references therein). Using our measurements of luminosities of $L_{1350\text{\AA}}$ and L_{CIV} for 33 reverberation mapping AGNs, we got $\alpha = 0.94 \pm 0.06$. Given $R_{BLR} \propto L_{CIV}^{0.60 \pm 0.16}$ as in Eq. (2), we can easily derive $R_{BLR} \propto L_{1350\text{\AA}}^{0.56}$, which is exactly shown in Eq.(4).

Exclusion of four radio loud objects ($R > 10$) from the 35 AGNs in the reverberation sample in Kaspi et al. (2005), i.e. 3C 120, 3C390.3, IC 4329A and PG 1226+023, only causes a small change for the slope of $R - L$ relations derived by Kaspi et al. (2005) and by us, because the sample is dominated by 31 radio quiet objects (Nelson 2000).

3.2 Black hole mass estimate and calibration

The mass of a black hole can be determined by the R_{BLR} and the velocity at this radius. The best is to use the time delay of variation of the $H\beta$ line to determine the R_{BLR} , and also use the $H\beta$ line-width for the velocity estimate. In this paper, to estimate the black hole mass, we will use the R_{BLR} calculated from luminosities of MgII and CIV lines using Eq. (1) and Eq. (2), which are ‘‘calibrated’’ from the measurements of $H\beta$ line, and also use the FWHM of MgII and CIV lines for the velocity estimates. Note that the time lags of flux variations of different emission lines related to that of the UV/optical continuum are different, as shown from the measurements of the reverberation AGNs (Peterson et al. 2000, 2005; Onken & Peterson 2002; Korista et al. 1995). For example, the time lag for the CIV line variation of NGC 5548 is approximately half of that for the $H\beta$ line, which

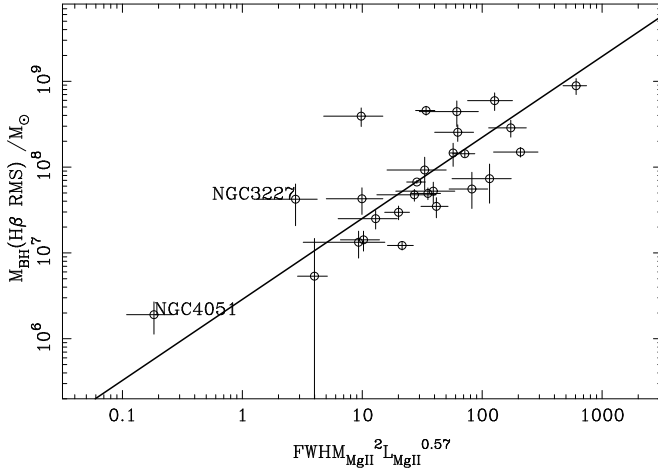


Fig. 3 The black hole masses of 27 reverberation AGNs derived from the $H\beta$ emission line from Peterson et al. (2004) versus the “mode” black hole masses from the FWHM and luminosity of $MgII$ emission line. The slope of the line is 0.94 ± 0.15 from an OLS bisector fit, and the correlation coefficient is 0.76. Here the $FWHM_{MgII}$ is in units of 1000 km s^{-1} , and L_{MgII} in units of $10^{42} \text{ erg s}^{-1}$.

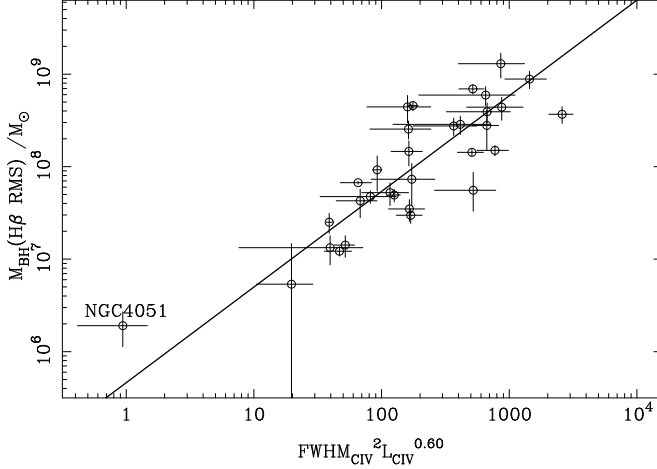


Fig. 4 Same as Fig. 3 but for CIV emission lines of 33 reverberation AGNs. The slope of the line is 1.0 ± 0.16 from an OLS bisector fit, and the correlation coefficient is 0.86.

indicates that the different emission lines are probably emitted at the different distances from the center of an AGN. Therefore we need to “calibrate” relations for black hole mass estimation when we have R_{BLR} and V from different emission lines.

Similar to Vestergaard (2002), we can estimate R_{BLR} from the line luminosity of either L_{MgII} or L_{CIV} (see Eq. (1) – Eq. (2)), and the velocity from the FWHM of $MgII$ or CIV . Finally we estimate the black hole masses from the R_{BLR} and FWHM value.

Using the known black hole masses of the reverberation AGNs in Peterson et al. (2004), we obtained the “calibrated” relations (shown in Fig. 3 and Fig. 4) for black hole masses as the following:

$$M_{BH}(MgII) = 2.9 \times 10^6 \left(\frac{L_{MgII}}{10^{42} \text{ergs}^{-1}} \right)^{0.57 \pm 0.12} \left[\frac{\text{FWHM}_{MgII}}{1000 \text{kms}^{-1}} \right]^2 M_{\odot}, \quad (5)$$

$$M_{BH}(CIV) = 4.6 \times 10^5 \left(\frac{L_{CIV}}{10^{42} \text{ergs}^{-1}} \right)^{0.60 \pm 0.16} \left[\frac{\text{FWHM}_{CIV}}{1000 \text{kms}^{-1}} \right]^2 M_{\odot}. \quad (6)$$

We also tried to estimate the black hole masses using the R_{BLR} estimated from continuum luminosities at 3000 \AA and 1350 \AA and the FWHM of MgII and CIV lines. We got the following relations:

$$M_{BH}(3000 \text{ \AA}) = 3.4 \times 10^6 \left(\frac{\lambda L_{3000 \text{ \AA}}}{10^{44} \text{erg s}^{-1}} \right)^{0.58 \pm 0.10} \left[\frac{\text{FWHM}_{MgII}}{1000 \text{ km s}^{-1}} \right]^2 M_{\odot}, \quad (7)$$

$$M_{BH}(1350 \text{ \AA}) = 1.3 \times 10^6 \left(\frac{\lambda L_{1350 \text{ \AA}}}{10^{44} \text{erg s}^{-1}} \right)^{0.56 \pm 0.12} \left[\frac{\text{FWHM}_{CIV}}{1000 \text{ km s}^{-1}} \right]^2 M_{\odot}. \quad (8)$$

Note Eq.(7) is similar to the Eq.(7) in McLure & Jarvis (2002) who obtained $M_{BH}(3000 \text{ \AA}) \propto L_{3000 \text{ \AA}}^{0.47} \text{FWHM}_{MgII}^2$. Our slope obtained with 27 reverberation mapping AGNs is slightly larger than that they obtained with 22 objects. Eq.(6) and Eq.(8) are very useful to calculate black hole masses of high redshift AGNs. Vestergaard (2002) has tried to do it using the R_{BLR} estimated from the continuum luminosity at 1350 \AA and the FWHM of CIV line, adopting $R_{BLR} \propto (\lambda L_{1350 \text{ \AA}})^{0.7}$. The black hole mass we obtained using Eq.(8) is slightly lower than that Vestergaard (2002) derived, but consistent with each other within one order of magnitude.

4 BLACK HOLE MASS ESTIMATION FOR SEVERAL AGN SAMPLES

The relations obtained in last section for UV lines can be used to estimate black hole masses of high redshift AGNs. For radio loud objects, as argued in Wu et al. (2004), jets could affect the estimate of R_{BLR} from the continuum luminosities. Therefore, our relations in Eqs. (1), (2), (5) and (6) based on the line luminosity for R_{BLR} should give better estimates of black hole masses for radio loud AGNs than those based on the continuum luminosities.

We apply the relations obtained above to estimate the black hole masses of AGNs in two samples. The first one is the Large Bright Quasar Survey (LBQS) sample (Forster et al. 2001; Hewett et al. 1995; Hewett et al. 2001). The second one is a composite radio-loud AGN sample (Cao & Jiang 1999; Celotti et al. 1997; Barthel et al. 1990; Constantin et al. 2002).

4.1 Data for LBQS sample

Forster et al. (2001) measured the optical/UV continuum and emission line properties of a homogeneous sample of 993 quasars in the LBQS, including the FWHM and equivalent width of lines, the flux and slope of continuum. The continuum fluxes have been Galactic extinction corrected. There are 504 objects with MgII line measurements and 403 objects with CIV line measurement. The black hole masses of these quasars can be estimated using the relations presented in Section 3. The continuum luminosities were calculated after K-correction according to the continuum slope. The line luminosities were calculated from the equivalent width of the emission line.

We also obtained the radio-loudness for these quasars. Radio-loudness is originally defined as the ratio between the radio flux density at 5 GHz and optical flux density at B band (4400 Å) (Kellermann et al. 1989). We adopt B_J magnitude (Hewett et al. 1995) as an approximation of B band magnitude, which only yields an increase of 0.03 in $\log R$ on average as Hewett et al. (2001) got the mean $B - B_J \simeq 0.07$. The optical luminosity at 4400 Å at the rest frame of a source were calculated by assuming an optical continuum slope of 0.3 ($f_\nu \propto \nu^{-\alpha}$, Schmidt & Green 1983). For radio data, we made the cross-identifications of quasars to sources in the catalog of the NRAO VLA Sky Survey (Condon et al. 1998) and found radio counterparts for 84 quasars with MgII line measurements and 60 quasars with CIV line measurements. The flux density observed at 1.4 GHz was then scaled to flux at 5 GHz at the rest frame of a source by roughly assuming a radio continuum slope of 0.5. So-obtained optical and radio data were used to calculate the radio loudness.

4.2 Data for a composited sample of radio loud AGNs

Celotti et al. (1997) collected a radio-loud sample to investigate the relation between the broad-line emission and the central engine of AGNs. Similarly, Cao & Jiang (1999) assembled a sample of radio-loud quasars and BL Lac objects from 1 – JY S4 and S5 radio source catalogs to investigate the relations between the broad emission line luminosity and jet power. Barthel et al. (1990) presented optical spectra of 67 radio-loud quasars ($1.5 < z_{em} < 3.8$) and measured the line properties, including MgII and CIV lines. Recently Constantin et al. (2002) observed the CIV emission line properties of 34 quasars at high-redshift ($z > 4$).

Using all these data, we composite a sample of radio-loud AGNs. We thus got 126 radio-loud AGNs with the MgII line luminosity and 164 AGNs with the CIV line luminosity. While, the FWHM data of the MgII line are only available for 86 objects, and CIV line for 92 objects. The radio-loudness of these AGNs were estimated using the data of 5 GHz flux density and absolute magnitude M_B available in the catalog of Véron-Cetty & Véron (2003). Optical flux densities were corrected for extinction using the A_B value

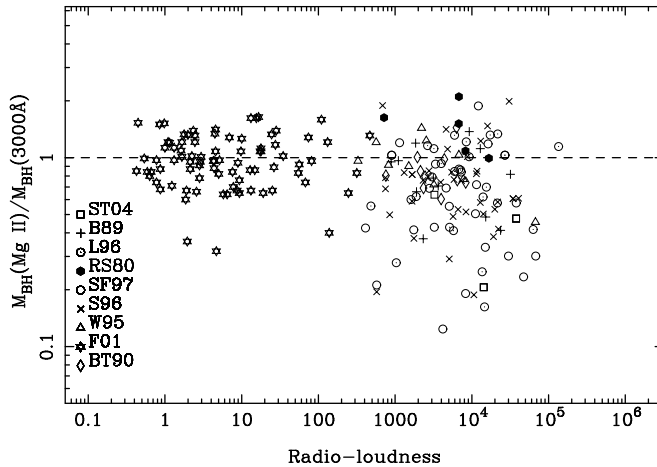


Fig. 5 The ratio of black hole masses estimated from the luminosities of MgII and continuum versus radio-loudness for 210 AGNs. Different symbols indicate objects from different references: Sbarufatti et al. (2004, ST04); Baldwin Wampler & Gaskell (1989, B89); Lawrence et al. (1996, L96); Richstone & Schmidt (1980, RS80); Scarpa & Falomo (1997, SF97); Stickel & Kuehr (1996, S96); Wills et al. (1995, W95); Forster et al. (2001, F01); Barthel, Tytler & Thomson (1990, BT90). The dashed line indicates the identical black hole masses. $z > 1.0$.

available from NED, and also K-corrected assuming an optical spectral index of 0.3. Radio flux density is also K-corrected assuming a slope of 0.5 if no radio spectral index is available in literature.

4.3 Black hole masses from the $R_{\text{BLR}} - L_{\text{MgII}}$ and $R_{\text{BLR}} - \lambda L_{\lambda}(3000\text{\AA})$ relations

We got 210 AGNs with the MgII measurements from two samples. But $M_{\text{BH}}(\text{MgII})$ and $M_{\text{BH}}(3000\text{\AA})$ can be estimated using the relations in Eqs. (1),(3),(5) and (7) for 170 objects of them having the available FWHM data of the MgII line.

Now we investigate the correlation between the mass ratio, $M_{\text{BH}}(\text{MgII})/M_{\text{BH}}(3000\text{\AA})$, and the radio-loudness for the 210 AGNs. For this purpose, the FWHM data are not necessary because $M_{\text{BH}}(\text{MgII})/M_{\text{BH}}(3000\text{\AA})$ calculated from Eqs. (5) and (7) only depends on the ratio of L_{MgII} and $L_{3000\text{\AA}}$. As shown in Fig. 5, when the radio-loudness is small, black hole masses estimated from luminosities of line and continuum are statistically identical. When the radio-loudness increases, the mass ratio tends to be more scattered and systematically lower than 1.0. Specifically, the mass ratio is less than 0.4 for five BL Lac objects (S5 1803+78, 4C 56.27, PKS 0537-441, PKS 1144-379, PKS 2029+121). Fig. 6 shows the histogram of the $M_{\text{BH}}(\text{MgII})/M_{\text{BH}}(3000\text{\AA})$ of the 154 radio-loud AGNs.

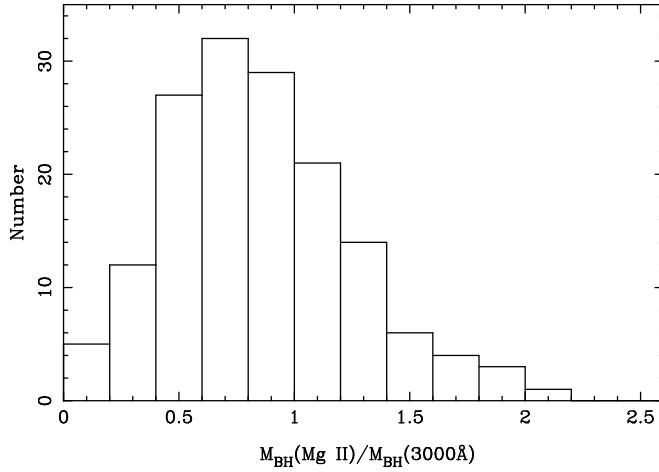


Fig. 6 Histogram of $M_{\text{MgII}}/M_{\text{BH}}(3000\text{\AA})$ for the 154 radio-loud AGNs ($R > 10$) shown in Fig. 5. About 69% of the objects have the mass ratio less than 1. The average mass ratio is 0.80 with $\sigma = 0.1$.

The mass ratio on average is 0.80 with a deviation of $\sigma = 0.1$. This result from these two samples confirms the suggestion in Wu et al. (2004) that for radio-loud objects, especially extremely radio-loud AGNs, black hole masses should be estimated from the R_{BLR} - line luminosity relation.

4.4 Black hole masses from the $R_{\text{BLR}} - L_{\text{CIV}}$ and $R_{\text{BLR}} - \lambda L_{\lambda}(1350\text{\AA})$ relations

We got 224 AGNs with the CIV measurement from two samples. Similarly to the MgII sample, we can estimate the black hole masses for 152 objects which have the FWHM data of CIV line. To check the dependence of the mass ratio, $M_{\text{BH}}(\text{CIV})/M_{\text{BH}}(1350\text{\AA})$, on the radio-loudness, we can use all 224 AGNs, as shown in Fig. 7. Fig. 8 shows the histogram of $M_{\text{BH}}(\text{CIV})/M_{\text{BH}}(1350\text{\AA})$ for the radio-loud 181 AGNs ($R > 10$). Clearly the black hole masses estimated from the BLR size derived from the $R_{\text{BLR}} - \lambda L_{\lambda}(1350\text{\AA})$ relation are probably overestimated as about 70% of the objects in the sample have the mass ratio less than 1. The average mass ratio is 0.73 with $\sigma = 0.2$. Therefore, it is confirmed again that the continuum luminosity is not a good indication of ionizing luminosity due to the possible jet contribution.

5 DISCUSSIONS AND CONCLUSIONS

Black hole masses of AGNs can be estimated either from the relations between the BLR size and UV emission line luminosity or the relations between the BLR size and UV continuum luminosity. We have obtained the new empirical relations between the BLR

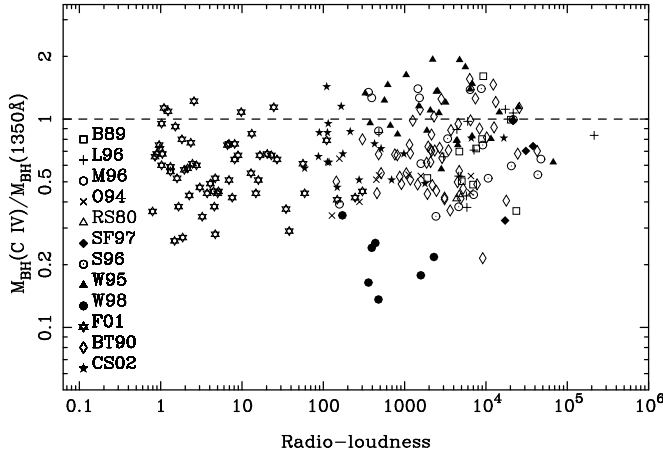


Fig. 7 Same as Fig. 5, but for 224 AGNs with measurement of CIV line. Different symbols indicate objects from different references: Baldwin Wampler & Gaskell (1989, B89); Lawrence et al. (1996, L96); Marziani et al. (1996, M96); Osmer, Porter & Green (1994, O94); Richstone & Schmidt (1980, RS80); Scarpa & Falomo (1997, SF97); Stickel & Kuehr (1996, S96); Wills et al. (1995, W95); Wang et al. (1998, W98); Forster et al. (2001, F01); Barthel, Tytler & Thomson (1990, BT90); Constantin et al. (2002, CS02). The ratio of the black hole masses were estimated from the $R_{\text{BLR}} - L_{\text{CIV}}$ and $R_{\text{BLR}} - \lambda L_{\lambda}(1350\text{\AA})$ relations.

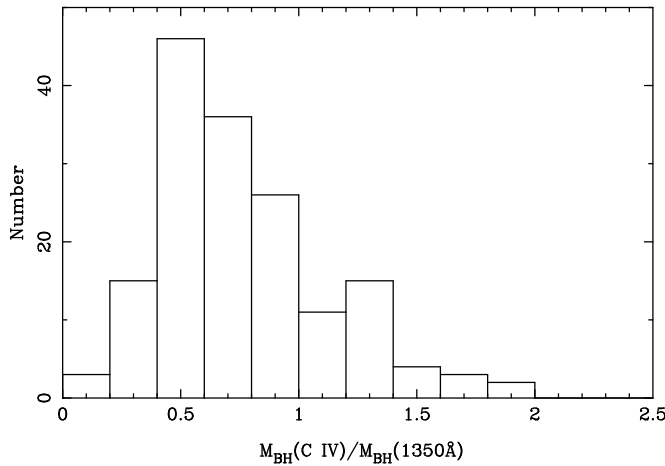


Fig. 8 Histogram of $M_{\text{BH}}(\text{Civ})/M_{1350\text{\AA}}$ for the 181 radio-loud AGNs ($R > 10$) shown in Fig. 7. About 70% of the objects have the mass ratio less than 1. The average mass ratio is 0.73 with $\sigma = 0.2$.

size and the MgII, CIV emission line luminosity from the reverberation-mapping AGNs (see Eq. (1), Eq. (2)). This enables us to estimate the black hole masses of high-redshift

($z > 0.8$) AGNs, using the luminosity and the FWHM of these UV emission lines (see Eq. (5), Eq. (6)).

The so-obtained black hole masses were compared to those obtained using the relations between the BLR size and UV continuum luminosity (see Eq. (7), Eq. (8)). For radio-loud AGNs, jets contribute substantially to the continuum luminosity, therefore the black hole masses estimated from the BLR size - continuum luminosity relations (Eq. (3), Eq. (4)) are probably overestimated. The relation of $R_{\text{BLR}} - L_{\text{CIV}}$ or that of $R_{\text{BLR}} - L_{\text{MgII}}$ should be a better choice.

For AGNs with the measurements of MgII lines, we have shown that $M_{\text{BH}}(\text{MgII})$ is very close to $M_{\text{BH}}(3000\text{\AA})$ when the radio-loudness is small. The black hole masses of radio loud AGNs estimated from the continuum luminosity are systematical larger than those from the line luminosity, confirming the suggestion by Wu et al. (2004) for $M_{\text{BH}}(\text{H}\beta) / M_{\text{BH}}(5100\text{\AA})$.

For AGNs with the measurements of CIV lines, our estimates for black hole masses of LBQS sample are slightly smaller than but still consistent with those estimated using the relations given by Vestergaard (2002), with a slope of 0.92 and a correlation coefficient of about 0.9. The distribution of the mass ratio does not show a strong correlation with the radio-loudness. We noticed that Baskin & Laor (2005) mentioned for the high ionization emission line like CIV the gravitational effects on the emission line shift and profile often can not be seen, while for low ionization line like MgII and H β this effects often can be seen. If this is true, it implies that the physics of high-ionization CIV emission lines may be different from the low ionization lines. Therefore, we should be cautious when estimating the black hole mass with CIV emission line properties.

We have compared the black hole masses of LBQS quasars estimated using Eq. (5) and Eq. (6) with those obtained by McLure & Jarvis (2002) and Vestergaard (2002). Fig. 9 and Fig. 10 show the comparisons of these results. Our estimates are systematically larger than those in McLure & Jarvis (2002) and smaller than those in Vestergaard (2001). This mainly comes from the different slopes of the R-L relations used in these studies.

It is important to understand the uncertainties of data used to obtain the relations presented in this paper. These uncertainties come from the errors of the measured BLR size, the variation of emission line flux and the line FWHM, and the different inclination of the BLR. These factors have been already discussed by Wu & Liu (2004). The BLR inclination will not affect the results in this work since the black hole mass ratio $M_{\text{BH}}(\text{MgII}) / M_{\text{BH}}(3000\text{\AA})$ and $M_{\text{BH}}(\text{CIV}) / M_{\text{BH}}(1350\text{\AA})$ has nothing to do with inclination. The plots for the BLR size and luminosity seem to have a larger scatter for lower luminosity objects (see Fig. (1) and Fig. (2)), which can also be seen in previous studies (Kaspi et al. 2000; Wu et al. 2004). More data of the low luminosity AGNs, especially with fu-

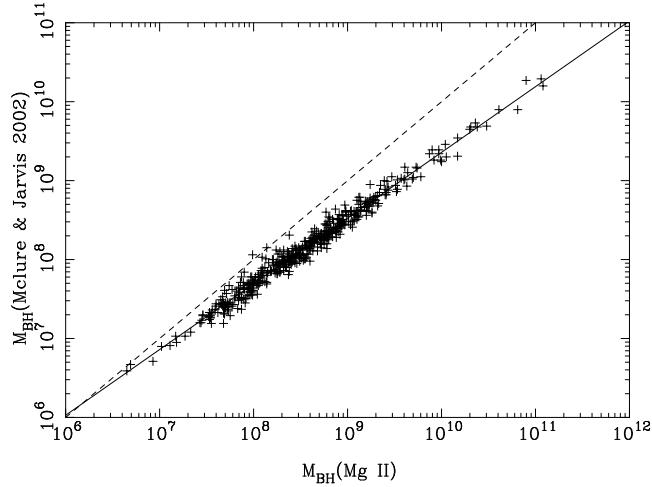


Fig. 9 Comparison of black hole masses estimated from luminosity of MgII (our Eq.(5)) and continuum at 3000\AA (McLure & Jarvis 2002) using LBQS sample. 476 objects were used which $1000\text{ km s}^{-1} < \text{FWHM}_{\text{MgII}} < 10000\text{ km s}^{-1}$ for avoiding measurement errors or narrow line contamination. The linear fit gives a slope of 0.83 (solid line) with a coefficients of 0.99. The dashed line indicates the equal masses from two approaches.

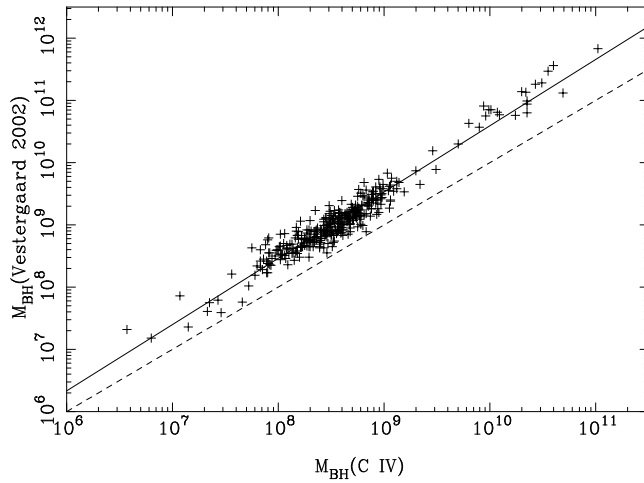


Fig. 10 Same as Fig 9 but for black hole masses estimated from luminosity of C IV (our Eq.(6)) and continuum at 1350\AA (Vestergaard 2002) with 341 objects plotted. The slope of the fit (solid line) is 1.06 and the correlation coefficients is 0.96.

ture reverberation mapping measurements, should be collected to improve the suggested relations.

Recently, more and more high redshift or high luminous quasars or radio-loud ones have been found. Because recent studies have used such $R - L$ relations to obtain black

hole masses of high redshift quasars with $4 \leq z \leq 6$ (Vestergaard 2004), including the most distant quasar SDSSJ114816.64 + 525150.3 ($z = 6.4$) (Willott, McLure & Jarvis 2003; Barth et al. 2003). However, the relations for R_{BLR} in Eq.(1,2,3,4) were obtained from the AGNs in reverberation sample, most of which are not very luminous and radio-quiet AGNs. We need to be caution if the black hole masses of these high redshift quasars are overestimated, especially when they are radio-loud objects. Indeed, a few high- z quasars have been already identified as radio-loud quasars (Fan et al. 2001; Momjian, Petric & Carilli 2004) therefore, further checks on the validity of suggested R-L relations for AGNs at high redshift or with large luminosity ones or large radio-loudness are still needed.

ACKNOWLEDGEMENTS

We thank Dr. Marianne Vestergaard for kindly providing us her iron template data in the UV band, and Dr. Michael Corbin for useful suggestions on the template and sending us his iron template spectra around 3000\AA . KMZ is grateful to Xiaohui Sun, Jing Wang, Yong Zhang and Yougang Wang for their numerous helps on fitting the spectra. XBW is supported by the National Natural Science Foundation of China (No. 10473001 & No. 10525313) and the Research Fund for the Doctoral program of Higher Education (No. 20050001026). JLH is supported by the National Natural Science Foundation of China (10025313) and the National Key Basic Research Science Foundation of China (G19990754) as well as the partner group of MPIfR at the National Astronomical Observatories of China. This work is based on the INES data from *IUE* satellite and the data from *HST* satellite partly. This research has made use of the NASA/IPAC Extragalactic Database (NED) which is operated by the Jet Propulsion Laboratory, California Institute of Technology, under contract with the National Aeronautics and Space Administration.

References

- Baldwin J. A. 1977, ApJ, 214, 679
 Baldwin J. A., Wampler E. J., & Gaskell C. M. 1989, ApJ, 338, 630
 Barth A. J., Martini P., Nelson C. H., et al. 2003, ApJ, 594, 95
 Barthel P. D., Tytler D. R., & Thomson B. 1990, A&AS, 82, 339
 Baskin A., & Laor A. 2005, MNRAS, 356, 1029
 Blandford R. D., & McKee C. F. 1982, ApJ, 255, 419
 Boroson T. A., & Green R. F. 1992, ApJS, 107, 69
 Cao X. W., & Jiang D. R. 1999, MNRAS, 307, 802
 Cardelli J. A., Clayton G. C., & Mathis J. S. 1989, ApJ, 345, 245
 Celotti A., Padovani P., & Ghisellini G. 1997, MNRAS, 286, 415
 Condon J. J., Cotton W. D., Greisen E. W., et al. 1998, AJ, 115, 1693
 Constantin A., Shields J. C., Hamann F., et al. 2002, ApJ, 565, 50
 Corbin M. R., & Boroson T. A. 1996 ApJS, 80, 109
 Fan X. H., Narayanan V. K., Lupton R. H., et al. 2001, AJ, 122, 2833

- Forster K., Green P. J., Aldcroft T. L., et al. 2001, *ApJS*, 134, 35
- Fromerth M. J., & Melia F. 2000, *ApJ*, 533, 172
- Hewett P. C., Foltz C. B., & Chaffee F. H. 1995, *AJ*, 109, 1498
- Hewett P. C., Foltz C. B., & Chaffee F. H. 2001, *AJ*, 122, 518
- Horne K., Peterson B. M., Collier S. J., et al. 2004, *PASP*, 116, 465
- Isobe T., Feigelson E. D., Akritas M. G., et al. 1990, *ApJ*, 364, 104
- Jester S. 2003, *New Astron. Rev.*, 47, 427
- Kapahi V. K., Athreya R. M., Subrahmanya C. R., et al. 1998, *ApJS*, 118, 327
- Kaspi S., Smith P. S., Netzer H., et al. 2000, *ApJ*, 533, 631
- Kaspi S., Maoz D., Netzer H., et al. 2005, *ApJ*, 629, 61
- Kellermann K. I., Sramek R., Schmidt M., et al. 1989, *AJ*, 98, 1195
- Korista K. T., Alloin D., Barr P., et al. 1995, *ApJS*, 97, 285
- Kuraszkiewicz J. K., Green P. J., Forster K., et al. 2002, *ApJS*, 143, 257
- Laor A. 2000, *ApJ*, 543, L111
- Lawrence C. R., Zucker J. R., Readhead A. C. S., et al. 1996, *ApJS*, 107, 541
- Marziani P., Sulentic J. W., Dultzin-Hacyan D., Calvani M., Mole M. 1996, *ApJS*, 104, 37
- McLure R. J., & Dunlop J. S. 2001, *MNRAS*, 327, 199
- McLure R. J., & Jarvis M. J. 2002, *MNRAS*, 337, 109
- McLure R. J., & Dunlop J.S. 2004, *MNRAS*, 352, 1390
- Momjian E., Petric A., & Carilli C. L. 2004, *AJ*, 127, 587
- Nelson C. H. 2000, *ApJ*, 544, L91
- O’Dea C. P., De Vries W., Biretta J. A., et al. 1999, *AJ*, 117, 1143
- Onken C. A., & Peterson B. M. *ApJ*, 2002, 572, 746
- Osmer P. S., Porter A. C., & Green R. F. 1994, *ApJ*, 436, 678
- Parma P., De Ruiter H. R., Capetti A., et al. 2003, *A&A*, 397, 127
- Peterson B. M. 1993, *PASP*, 105, 247
- Peterson B. M. 1997, *An Introduction to Active Galactic Nuclei*, Cambridge, p.91
- Peterson B. M., Wanders I., Bertram R., et al. 1998, *ApJ*, 501, 82
- Peterson B. M., & Wandel A. 1999, *ApJ*, 521, L95
- Peterson B. M., & Wandel A. 2000, *ApJ*, 540, L13
- Peterson B. M., Berlind P., Bertram R., et al. 2002, *ApJ*, 581, 197
- Peterson B. M., Ferrarese L., Gilbert K. M., et al. 2004, *ApJ*, 613, 682
- Richstone D. O., & Schmidt M. 1980, *ApJ*, 235, 361
- Santos-Lleo M., Clavel J., Schulz B., et al. 2001, *A&A*, 369, 57
- Sbarufatti R., Treves A., Falomo R., et al. 2004, *astro-ph/0410692*
- Scarpa R., & Falomo R. 1997, *A&A*, 325, 109
- Scarpa R., Urry C. M., Falomo R., et al. 1999, *ApJ*, 526, 643
- Scarpa R., & Urry C. M. 2002, *New Astron. Rev.*, 46, 405
- Schmidt M., & Green R. F. 1983, *ApJ*, 269, 352
- Stickel M., & Kuehr H. 1996, *A&AS*, 115, 11
- Véron-Cetty M. P., & Véron P. 2003, *A&A*, 412, 399
- Vestergaard M., & Wilkes B. J. 2001, *ApJS*, 134, 1
- Vestergaard M. 2002, *ApJ*, 571, 733
- Vestergaard M. 2004, *ApJ*, 601, 676
- Wandel A., Peterson B. M., & Malkan M. A. 1999, *ApJ*, 526, 579
- Wandel A. 2002, *ApJ*, 565, 762
- Wang T.-G., Lu Y.-J., & Zhou Y.-Y. 1998, *ApJ*, 493, 1
- Wills B. J., Thompson K. L., Han M., et al. 1995, *ApJ*, 447, 139
- Willott C. J., McLure R. J., & Jarvis M. J. *ApJ*, 2003, 587, L15
- Wu X.-B., & Han J. L. *ApJ*, 2001, 561, L59
- Wu X.-B., & Liu F. K. *ApJ*, 2004, 614, 91
- Wu X.-B., Wang R., Kong M. Z., et al. 2004, *A&A*, 424, 793
- Zhang T. Z., Wu X. B., 2002, *ChJAA*, 2, 487

Table 1 Parameters of MgII , CIV emission lines for 35 AGNs of reverberation-mapping AGN sample.

Object	R _{BLR} (lt-days)	M _{BH} 10 ⁶ M _⊙	FWHM _{Mgii} (km s ⁻¹)	L _{Mgii} (10 ⁴² erg s ⁻¹)	L _{3000Å} (10 ⁴⁴ erg s ⁻¹)	FWHM _{Civ} (km s ⁻¹)	L _{Civ} (10 ⁴² erg s ⁻¹)	L _{1350Å} (10 ⁴⁴ erg s ⁻¹)	Num MgII	Num CIV
(1)	(2)	(3)	(4)	(5)	(6)	(7)	(8)	(9)	(10)	(11)
3C120	38.1 ^{+21.3} _{-15.3}	55.5 ^{+31.4} _{-22.5}	3740±538	22.57±2.64	10.44±2.63	4652±937	206.81±34.22	34.30±10.05	13	34
3C390.3	23.6 ^{+6.2} _{-6.7}	287±64	8174±622	5.36±1.83	0.99±0.48	7884±1870	23.91±9.14	2.41±1.30	6	92
Akn120	42.1 ^{+7.1} _{-7.1}	150±19	5727±842	25.93±4.94	15.45±3.10	6134±603	157.83±20.76	46.75±10.21	20	37
F9	17.4 ^{+3.2} _{-4.3}	255±56	4682±547	6.31±1.38	2.94±0.93	4981±782	23.23±7.24	3.67±2.27	54	106
MRK79	11.7 ^{+5.2} _{-5.2}	52.4±14.4	5072±1014	2.09±0.42	0.80±0.24	5301±858	10.80±1.36	1.92±0.74	1	4
MRK110	26.0 ^{+6.6} _{-6.6}	25.1±6.1	2878±575	2.19±0.44	0.55±0.16	3283± 33	8.59±0.45	0.67±0.01	2	2
MRK279	12.4 ^{+6.0} _{-6.0}	34.9±9.2	5346±465	1.92±0.27	1.04±0.47	7306±853	6.63±0.91	1.06±0.44	6	16
MRK335	14.6 ^{+3.0} _{-3.0}	14.2±3.7	2700±346	1.82±0.32	1.77±0.23	3419±202	12.17±1.27	2.64±0.41	17	22
MRK509	79.6 ^{+6.1} _{-5.4}	143±12	3921±272	15.03±1.87	7.36±1.37	6138±537	78.66±7.43	13.39±2.92	33	50
MRK590	23.2 ^{+7.3} _{-7.3}	47.5±7.4	5324±1064	0.93±0.19	0.15±0.05	4477±441	10.50±7.01	0.85±0.71	1	2
MRK817	22.6 ^{+9.7} _{-9.7}	49.4±7.7	5112±601	1.69±0.12	1.07±0.04	6481±236	6.27±0.44	1.28±0.13	2	3
NGC3227	6.8 ^{+2.0} _{-2.0}	42.2±21.4	5406±1081	0.02±0.00	0.01±0.00	1	0
NGC3516	6.7 ^{+6.8} _{-3.8}	42.7±14.6	5036±900	0.19±0.05	0.15±0.05	8018±681	1.10±0.33	0.19±0.09	19	76
NGC3783	10.2 ^{+3.3} _{-2.3}	29.8±5.4	3031±235	3.96±0.54	2.03±0.50	4320±329	40.13±5.10	8.35±2.23	97	76
NGC4051	5.8 ^{+2.6} _{-1.8}	1.91±0.78	2273±350	0.003±0.001	0.004±0.001	4337±898	0.01±0.002	0.002±0.0004	8	19
NGC4151	7.3 ^{+5.9} _{-5.9}	13.3±4.6	5866±1342	0.10±0.03	0.06±0.04	6939±1902	0.72±0.31	0.07±0.05	416	454
NGC4593	1.2 ^{+9.2} _{-5.3}	5.36 ^{+9.37} _{-6.95}	3613±363	0.12±0.02	0.08±0.02	5983±939	0.37±0.09	0.05±0.02	13	25
NGC5548	16.2 ^{+5.8} _{-5.8}	67.1±2.6	5394±288	0.97±0.12	0.36±0.10	5289±421	4.15±0.80	0.41±0.38	116	179
NGC7469	4.5 ^{+0.7} _{-0.8}	12.2±1.4	4123±284	1.51±0.28	0.81±0.20	4402±352	4.38±0.60	1.06±0.17	11	229
PG0026+129	111.0 ^{+24.1} _{-28.3}	393±96	1714±342	8.33±1.67	19.27±5.78	7131±1426	75.22±15.04	23.28±6.98	1	1 ^a
PG0052+251	89.8 ^{+24.5} _{-24.1}	369±76	9380±690	289.44±32.21	29.74±2.25	0	2
PG0804+761	146.9 ^{+18.8} _{-18.9}	693±83	5276±342	134.24±20.95	29.28±4.62	0	2
PG0844+349	3.0 ^{+12.4} _{-10.0}	92.4±38.1	3759±751	4.48±0.90	4.61±1.38	4237± 60	15.56±1.42	5.77±0.08	1 ^a	2
PG0953+415	150.1 ^{+21.6} _{-22.6}	276±59	3987±797	192.41±38.48	45.61±13.68	0	1 ^a